Research Square

Preprints are preliminary reports that have not undergone peer review.
They should not be considered conclusive, used to inform clinical practice,
or referenced by the media as validated information.

Recovery and characterization of nanocellulose from Phalaris aquatica L. energy crop: towards the Mediterranean biorefineries sustainability and biodiversity valorisation.

Ioannis Pappas

io.pappas@thessaly.gov.gr

Department of Plant Production, Administration of Rural Economy P.E. Larissas,

Emmanouil Papaioannou

Lancaster University

Research Article

Keywords: Phalaris aquatica L., Cellulose nanocrystals, Biodiversity, Biorefinery, Biodegradable materials

Posted Date: May 25th, 2026

DOI: https://doi.org/10.21203/rs.3.rs-8433646/v1

License: This work is licensed under a Creative Commons Attribution 4.0 International License.
Read Full License

Additional Declarations: No competing interests reported.

Abstract

Phalaris aquatica L. is a perennial species native in the Mediterranean region. It is considered as a sustainable energy crop and its part of this area biodiversity. This study presents evidence for nanocellulose extraction from this crop by low concentration alkali (4% w/v NaOH) and bleaching (1.7% w/v acetic acid, aqueous chlorite) treatments, followed by an acid hydrolysis with sulfuric acid. The effects for each of these processes' on the recovered nanocellulose properties are recorded, providing evidence of the effect of each stage on their recovery. The chemical composition of the fibres revealed an increase of cellulose content from raw (43.1% w/w) to final acid treated fibres (90.5% w/w). FT-IR, TG, DSC analysis confirms the removal of hemicellulose and lignin from these fibres and the improved thermal properties of the recovered nanocellulose, as well as a high crystallinity index (76.1%, XRD results). DLS analysis revealed an average nanocellulose aggregates particle size of 165.2 ±15.4 nm, while Atomic Force Microscopy (AFM) morphology measurements support further this aggregates size.These nanocellulose traits has a substantial potential as reinforcement agent in nanocomposites with diverse innovative industrial and biomedical applications.

1. Introduction

European Union Biodiversity Strategy for 2030 promotes the sustainable resource management, through biodiversity valorisation (European Commission 2020). This approach encourages the use of natural resources, ensuring that economic activities impact on biodiversity and ecosystems services is neutral or even positive. This biodiversity strategy can drive innovation in areas like sustainable agriculture, renewable energy, and circular economy, promoting solutions that benefit economy, society and environment (Viti et al. 2024).

The use of materials for industrial applications that are renewable is substantially increasing, driven by the exponential demand for alternatives to fossil-based chemicals. The late resources are considered finite and with a proven negative environmental impact. In this context, cellulose, which is the most abundant natural biodegradable biopolymer on earth, can serve as source for CNCs. CNCs is a promising material currently under intense research interest (Brinchi et al. 2013). CNCs offers numerous advantages, such as renewability, high specific strength, modulus, biodegradability, biocompatibility, low toxicity and less susceptibility to fracture during processing (Ljungberg et al. 2006). Owing to these features, CNCs can be used as a high-quality reinforcing filler for polymers and biodegradable materials (Patil et al. 2022; Zhang et al. 2023; Langari et al. 2023). CNCs is isolated from various lignocellulosic biomass resources by enzymatic, chemical, and mechanical methods. Chemical methods for CNCs extraction from lignocellulosic biomass include three sequential steps for the removal of the amorphous components such as: a) alkali treatment (hemicellulose removal), b) bleaching treatment (lignin removal) and c) concentrated acid hydrolysis (sulfuric & hydrochloric; amorphous cellulose removal). CNCs refers to a variety of cellulose-based materials with at least one dimension on the nanoscale (Carter et al. 2021). These CNCs materials composed of crystalline and/or amorphous regions with fibre diameters less than 100 nm and fibre lengths less than or equal to several microns (Mokhena and John

2020). Thus the understanding of biomass structure is crucial for CNCs production, since cell wall content (cellulose, hemicellulose and lignin) of lignocellulosic biomass varies among species, plant fraction and growth conditions (Brinchi et al. 2013; Pires et al. 2019).

Several lignocellulosic biomasses have been reported as natural sources for CNCs production, such as agricultural, industrial residues, annual fibre crops, wood and energy crops. These biomasses originate from agricultural and industrial residues, such as rice husk (Johar et al. 2012), rice straw (Jiang and Hsieh 2013), raw banana, jute and pineapple leaf fibres (Abraham et al. 2011), corn cob (Silverio et al. 2013), sugarcane bagasse (Mandal and Chakrabarty 2011), soy hulls (Flauzino Neto et al. 2013; Velázquez et al. 2022), mulberry bark (Li et al. 2009), maize straw (Rehman et al. 2014), coconut husk (Rosa et al. 2010; Abraham et al. 2013), wheat straw (Kaushik et al. 2013; Trivedi et al. 2023), oil palm empty-fruit-bunch (Fahma et al., 2010). Annual fibre crops such as sisal (Moran et al., 2008), hemp (Le Troedec et al. 2008; Pascoli et al. 2023), kenaf (Kargarzadeh et al. 2012) and wood, such as hardwoods (Zhang et al. 2021), and softwoods have been used for NC production. There are limited studies about NC production from herbaceous species utilisation, such as perennial grasses (Lyons et al. 2013; Sucinda et al. 2020; Pascoli et al. 2023), and even less from perennial grass energy crop (Pires et al. 2022). The different composition of the cell wall components is a crucial parameter in evaluating the suitability of feedstock for CNCs production (Ghaemi et al. 2019). The lower lignin content in biomass feedstocks can be advantageous for CNCs extraction, potentially reducing the number of delignification steps required compared to feedstocks with higher lignin content (Srivastava et al. 2023).

Perennial grasses have been widely exploited for serving as second-generation bioethanol feedstocks', due to their agronomic high yield, high carbohydrates (cellulose and hemicellulose) composition, low lignin content, and their positive overall environmental and social performance (Sanderson and Adler 2008). Although, bioethanol is a sustainable alternative to petroleum as a transportation fuel, the economics of the production chain must be significantly improved before it's widely accepted. An alternative strategy is the simultaneous production of cellulosic ethanol and other added value materials, such as CNCs and phenolic acids. This approach can maximise the revenues and the economic sustainability of these perennial grasses utilisation (Oksman et al. 2011; Song et al. 2014). *Phalaris aquatica* L. was identified as a novel sustainable energy crop for the biorefinery industry, due to easy and high yield enzymatic saccharification, and the added value phenolic acids (Pappas 2010; Pappas et al. 2014; Pappas et al. 2023). CNCs recovery from *Phalaris aquatica* L. energy crop is currently absent from the literature.

Phalaris aquatica L. is a perennial cool season grass species native of the biodiversity of the Mediterranean region that has widely used as forage crop for the production of highly digestible biomass for livestock production in Greece (Dini-Papanastasi and Goulas 1995). In addition, this species has been fully adapted to the constrains of the Mediterranean climate type such as high air temperature, low and uneven rainfall incident especially in summer season (drought tolerance) and for the above reasons has been successfully introduced for cultivation in pastures of Australia. Phalaris (*Phalaris aquatica* L.) is the most important sown pasture grass species in southern Australia particularly where rainfall is too low or

unreliable for perennial ryegrass (*Lolium perenne* L.) (Norton et al. 2012). It is estimated to be an important component in about 2.7 million of hectares of pastures in Australia due to its good drought resistance (Oram et al. 2009). The low lignin content of the species biomass may require fewer delignification steps for the extraction of CNCs, compared to other feedstocks with higher lignin content (Pascoli et al. 2023). Lignin plays a key role in determining biomass recalcitrance in forage grasses (Oliveira et al. 2020).

This study's objectives were a) evaluate a sequence of relatively pre-treatment steps, namely low concentration alkali, bleaching and acid hydrolysis, on CNCs isolation from *Phalaris aquatica* L. and b) to characterise the CNCs properties, supporting their technological advantages.

2. Materials and Methods

2.1 Biomass feedstock

Biomass for this study, was obtained from a rainfed energy crop of *Phalaris aquatica* L. grown for four years at an experimental field at Pteleos site (39° 3' 0" N latitude and 22° 57' 0" E longtitude) of Thessaly Region in Central Greece (Pappas, 2010; Pappas et al., 2014; Pappas et al., 2023). The above biomass was harvested at the end of the growing season (end of July). Air-dried biomass with moisture content less than 6% w/w, was milled to a particle size (less than 1 mm) by using a laboratory hammer mill (Retch, Germany) and stored in plastic air tight sealed bags at room temperature, until further use.

2.2 Analytical methods

2.2.1 Cell wall composition of P. aquatica fibers

The cell walls composition of raw material was determined using Van Soest Fiber Analysis System (Van Soest et al., 1991). The neutral detergent fibre (NDF) was used to estimate the total lignocellulosic materials (cellulose, hemicellulose and lignin), while acid detergent fibre (ADF) and acid detergent lignin (ADL) was used to estimate the concentration of lignin and cellulose. Hemicellulose was determined by the difference (%NDF - %ADF) and cellulose by the difference (%ADF - %ADL). All experiments and analytical determinations were performed in duplicate and average results are presented, with the standard deviation being lower than 5% in all cases.

2.2.2 Alkali pre-treatment of P. aquatica fibres

The biomass was treated with a NaOH solution (4 w/v %) into a borosilicate screw cap bottle in a silicon oil bath at 80^{o}C for 2h, under agitation (300 rpm). This reaction stopped by quenching in cold water. The solid was filter and washed several times using distilled water until the washing water reached pH 7, in order to neutralise the fibres and to remove all the solubilized non-cellulosic components. Then the fibres were dried by using an incubator at 60 °C for 24 h.

2.2.3 Bleaching pre- treatment of P. aquatica fibres

Following NaOH treatment, the bleaching process was performed by adding a buffer solution of acetic acid, aqueous chlorite (1.7 w/v%) and distilled water under reflux (using a silicon oil bath at 80◦C) for 4 h. The mixture was allowed to cool, was filtered (filter Whatman 1) and washed using excess distilled water until a pH 7 was measured. Then these fibres were dried by using an incubator at 60 °C for 24 h.

2.2.4 Acid hydrolysis of P. aquatica fibres

The acid hydrolysis treatment was conducted with 5 w/v% pre-treated fibres (alkali and bleaching) at a temperature of 50◦C for 40 min under continuous stirring (300 rpm), using sulphuric acid 65% w/w (pre-heated). The solids after the hydrolysis were washed and centrifuged at 10,000 rpm at 10 ◦C for 10 min. This centrifugation step was repeated several times until the supernatant pH was constant in the range of 5-6. The resulting suspension was then sonicated for 2 min, freeze at -20◦C and then freeze-dried for 48 h before any further use.

2.3 Structural characterization of P. aquatica lignocellulosic biomass

2.3.1. FTIR analysis

For the Fourier Transform Infrared spectra acquisition a Schimadzu spectrometer (Japan) was used. 1.0 mg of raw, as well as each of the pre-treated, *P. aquatica* drybiomass were dispersed in 100 mg of spectroscopic grade KBr and subsequently pressed into disks at 10 MPa for 5 min. The spectra were obtained with an average of 25 scans and a resolution of 4 cm^{-1} in the range of 4000–400 cm^{-1}.

2.3.2 Thermogravimetric analysis (TGA)of biomass

A Thermal Gravimetric Analyzer (NETZSCH STA 44 F3 Jupiter, Germany) was used to characterize the thermal stability of the various cellulose samples. 2 mg of each dry sample was heated from 30◦C to 750◦C, at a heating rate of 10◦C/min. All measurements were performed under a nitrogen atmosphere, with a gas flow of 20 ml/min for preventing any thermoxidative degradation.

2.3.3. X-ray diffraction (XRD)of the biomass

Crystallinity of the initial and the pre-treated *P. aquatica* dry biomass were analysed using a X-pert pro diffractometer (PANalytical, Netherlands). Crystallinity Index (CrI) and crystallite size were calculated as per protocols adopted by Segal et al. (1959) and Oh et al. (2005). The scan scope was between 10^{o} and 30^{o} with a step size of 0.02^{o} and determination time was 1 s/0.02^{o}. The crystallinity index (CI) of biomass was calculated based on the empirical method (Segal et al., 1959) by the use of the following equation:

$$CrI = (I_{002} - I_{am})/I_{002} \times 100\%$$

where in I_{002} is the maximum intensity of the diffraction from the 002 plane, and I_{am} is the minimum intensity of the diffraction between peaks 101 and 002. The I_{002} is the crystalline area and $I_{am}$is the

amorphous area.

2.3.4. Differential Scanning Calorimetry (DSC) of the NC particles

This analysis was carried out in a Shimadzu DSC-50 (Japan) from room temperature to 400^{o}C, at a heating rate of 10^{o}C/ min, under nitrogen atmosphere. The thermograms were used to determine the glass transition temperature (T_g) and the melting temperature (T_m) in order to monitor the thermal behaviour and phase transition of the materials.

2.3.5 Particle size analysis by dynamic light scattering (DLS)

Particle size was measured using a Nano Size Particle Analyzer (ZEN 1600 MALVERN, USA) in the range between 0.6 nm and 6.0 μm, under the following conditions: particle refractive index 1.59, particle absorption coefficient 0.01, water refractive index 1.33, viscosity 0.8872 cP, temperature 25◦C and general calculation model for irregular particles. Twenty measurement cycles of 10 s each were taken, and the average particle size was calculated by using this instrument software (DTS, Ver. 5.00 from Malvern).

2.3.6. AFM analysis

Images of the CNF surface morphology were obtained using a Bruker Dimension Icon (AFM, Bruker, Billerica, MA, USA). Atomic force microscopy (AFM) analysis was performed in tapping mode, with a scan rate of 1 Hz on NC.

3. Results and Discussion

3.1 Compositional analysis of the fibres.

The chemical composition of raw, alkali treated and bleached *P. aquatica* lignocellulosic biomass is given in Table 1. Cellulose is the predominant component of raw *P. aquatica* lignocellulosic biomass containing 43.1% (w/w), followed by hemicellulose and a low lignin contents (25.8% w/w and 7.6 % w/w, respectively). The hemicellulose content is decreased after alkali treatment from 25.8% to 13.5 % w/w (~47.3% less concentration), indicating that NaOH treatment is removing effectively mainly hemicellulose and to lesser extent lignin (~14.7%). Based on chemical composition analysis lignin is removed by a large extend (93.8%) after the bleaching treatment, resulting in fibres with high cellulose content (90.5% w/w). Similar trends have been reported by recent studies working with different lignocellulosic feedstocks for NCC extraction (Li et al., 2009; Johar et al., 2012; Flauzino Neto et al., 2013; Abraham et al., 2013).

Table 1. Chemical composition (% w/w dry weight) of *Phalaris aquatica* L. fibres at the end of each stage of chemical treatment

3.2 FTIR profile of the various biomasses after each stage

Fig. 1. FTIR spectra of (a) raw biomass; (b) alkali treated; (c) bleached and (d) acid hydrolysed cellulose of *Phalaris aquatica*.

The FTIR spectra of raw and chemically treated *Phalaris aquatica* L. lignocellulosic biomass are shown in Figure 1. The C=O stretching vibration (at 1735 cm^{-1}) is attributed mainly to the acetyl and uronic ester groups of pectin, hemicellulose or the ester linkage of carboxylic group of ferulic and p-coumaric acids of lignin and/or hemicellulose (Hsu et al., 2010). This peak disappeared completely in the NaOH treated fibres, due to the removal of most of the hemicellulose and lignin. The aromatic C-O in plane symmetrical stretching vibration of aromatic ring present in lignin appeared at 1510 cm^{-1} (Li et al., 2009). The intensity of the peaks decreased in the lignin removal stage, which was attributed to the effective removal of lignin (Rosa et al., 2012). The absorbance peak observed in the spectra of fibres (raw, treated and nanocellulose) at 1649 cm^{-1} is attributed to the O–H bending of the adsorbed water (Le Troedec et al., 2008; Mandal &Chakrabarty 2011; Flauzino Neto et al.,2013). The peaks at 1061 and 897 cm^{-1} are associated with cellulose the C–O stretching and C–H rock vibrations of cellulose (Alemdar & Sain, 2008), which appeared in all of the spectra. These peaks in the treated samples appear with higher intensity, supporting this way the increase in of cellulose in them (Flauzino Neto et al., 2013).

3.3 Thermal properties of the biomass after each pre-treatment

The investigation of thermal properties of the natural fibres is important for evaluating their applicability in bio-based composite processing, where the processing temperature rises above 200^{o}C (for thermoplastic polymers). According to Jeguirim et al. (2010) the thermal degradability is affected by the chemical composition of raw biomass. Lignocellulosic materials based on their composition present different thermal behaviours.

Fig. 2 TG of (a) raw biomass; (b) alkali treated; (c) bleached and (d) acid hydrolyzed cellulose of *Phalaris aquatica*.

The TGA results obtained from *Phalaris aquatica* lignocellulosic biomass at different stages of chemical treatment are summarised in Figure 2. For all the examined biomasses, the weight loss observed at 35–150∘C was small, attributed to the evaporation of the residual water (moisture content) and volatile compounds of low molecular weight (naturally present in *Phalaris aquatica*) (Fahma et al., 2010; Flauzino Neto et al., 2013; Sucinda et al., 2020; Pappas et al., 2023). At elevated temperatures, a more intense weight loss was observed. The bleaching treatment induced materials with an increase thermal stability, in respect to raw and alkali treated biomasses. This trait attributed to lower decomposition temperature of hemicellulose and lignin, in the alkali treated *P. aquatica* biomass, as compared with those of cellulose (Moran et al., 2008) and their progressive removal improves the thermal stability of the remaining material. According to Yang et al. (2007) hemicellulose is easily degraded to volatiles at relatively low temperatures (220-315^{o}C) due to their amorphous structure and branching characteristics.

NC showed significantly different degradation behaviour from *P. aquatica* L. raw fibres. Lower start decomposition temperature at 180-330^{o}C and broader degradation temperature at 330-500^{o}C were noted, suggesting two degradation stages similar to those reported by Li et al. (2009); Flauzino et al. (2013); Abraham et al. (2013). The lower temperature stage corresponds to the degradation of more amorphous, and therefore more highly sulphated regions, whereas the higher temperature stage is related to the breakdown of unsulfured crystal groups emended dipper to the structure. Sulphated groups are introduced into the cellulose crystals during the sulfuric acid hydrolysis, and NC decreased thermostability in such cases is reported in the existing literature (Johar et al., 2012; Silverio et al., 2013; Benini et al., 2018). The residues remaining in the untreated and treated fibres after heating to 500^{o}C constitutes the presence of carbonaceous materials (Thiripura Sundari & Ramesh, 2012).

3.4 Crystallinity changes of biomass during the pre-treatments

The powder X-ray diffraction patterns of the raw and chemical treated cellulose fibres are presented in Figure 3. CrI of *P. aquatica* biomass increased with alkali, bleached and acid hydrolysis treatments (Table 2). During the alkali treatment CrI of raw biomass is increased from 59.1% to 66.3%. At the end of the bleaching treatment CrI is slightly increased by 1%. CrI is increased with NaOH and $NaOCl_2$ treatments and this explained from: (a) removal of amorphous components, such as hemicellulose and lignin (Rosa et al., 2010; Johar et al., 2012; Flauzino et al., 2013) and (b) rearrangement of the crystalline regions (Sghaier et al., 2012). The increase in CrI value of nanocellulose to 76.1% after acid hydrolysis in relation to raw biomass is within the reported by several studies range of values for various lignocellulosic feedstocks Li et al. (2009) (mulberry); Mandal & Chakrabarty, (2011) (sugarcane bagasse); Silverio et al., (2013) (corncob); Rehman et al., (2014) (maize straw); Jiang & Hsieh (2013) (rice straw), Benini et al. (2018) (*Imperata brasiliensis* grass), Sucinda et al., (2020) (tropical grass) indicating the effectiveness of the selected pre-treatment process. In the present study a reduction of the total stages in NaOH and $NaClO_2$ pre-treatment for nanocellulose production (Rosa et al. 2010; Johar et al., 2012) is achieved. This attributed to *P. aquatica* L. biomass feedstock's cell wall composition, especially due to its extremely low lignin content (<8%) and high initial crystallinity index. The higher crystallinity of the chemically treated cellulose fibres is associated with higher tensile strength of the fibres. Therefore, the expected mechanical properties of the composite material could be improved by using these nanofibers (Rosa et al., 2012).

Fig 3. X-ray diffraction patterns for (a) raw biomass, (b) NaOH (alkali)-treated biomass, (c) $NaClO_2$ (bleached) biomass and (d) acid hydrolysed cellulose.

Table 2. Crystallinity index (CrI) of *Phalaris aquatica* fibres at different stages of chemical treatment

3.5 Enthalpy changes during the pre-treatments

Fig. 4. DSC curve of (a) raw; (b) alkali treated, (c) bleached treated and (d) acid hydrolyzed cellulose.

The DSC diagrams of raw, alkali, bleached and nanocellulose are presented in Fig. 3. All thermograms from 30^{o}C to 140^{o}C present an endothermic peak due to water evaporation absorbed in the intercellular region of the fibre (Moran et al., 2008; Mandal & Chakrabarty, 2011). The raw biomass fibres have two exothermic peaks at the temperature range of 250-290◦C and 300-360◦C. The first peak is attributed to the decomposition of hemicellulose and a portion of lignin degradation, while the second is related to the intense degassing and combustion of volatiles parts (Kijo-Kleczkowska et al., 2022). Following alkali treatment this exothermic peak disappeared indicating that most of hemicellulose and lignin was removed from the fibre. In the temperature range of 315-370◦C in alkali treated fibre one broad endothermic appears, owing to the depolymerisation of cellulose with the formation of volatiles (Kabir et al., 2013). The same profile with alkali treatment is identified after the bleaching process of the fibres, with a slight lower endothermic peak at 360 ^{o}C. This is indicative of the lower degree of polymerization of cellulose polymer and the higher crystallinity index. Acid hydrolysis treated fibres exhibited a lower endothermic peak at 300.14^{o}C, corresponding to the combination of the crystalline part. The decrease of the position of the peak is due to the decrease of degree of polymerisation and crystallite length (Moran et al., 2008; Hamad & Hu, 2010) since the crystallinity index was increased (76.1%, Table 2). Thus, the thermal stability of the fibres increases during each processing step and the extracted NC has improved thermal properties.

3.6 Particle size of the NC fibres

Fig 5. Particle size distribution of NC aggregates obtained from *Phalaris aquatica* L. energy crop.

An almost Gaussian size distribution of water suspended NC particles by DLS is given in Figure 4. The result confirmed the dimension of the NC aggregate particles are in the range of 54 - 400 nm with an average value of 165.2 nm, while the percentage of NCC whose particles size less than 260 nm reaches ≈ 80%. The standard deviation for the particle sizing is 7.7 nm (5.5%) with a Chi Squared of 2.1 for Gaussian summary. Similar results are reported by Benini et al. (2018) for cellulose nanoparticles that produced from *Imperata brasiliensis* grass fibres and Sicunda et al. (2020) studied the extraction of nanocellulose from *Pennisetum purpureum* a tropical grass in Malaysia.

3.7 NF fibres topography

Fig 6. Atomic Force Microscopy (AFM) of acid hydrolyzed cellulose of *Phalaris aquatica* L.

According to Lou et al., (2023) AFM is used to produce the surface topology of biomass materials. In Figure 5 for the scanning of a 10 μm AFM image topography the NC aggregates represent a needle like structure with an average height from valley to top of 190.2 nm, which is close to the size reported in case of DLS measurements. In such images the bright areas attributed to crystalline regions, while darker areas are indicative of amorphous domains (Sathwane et al., 2024; Hoseinpour et al., 2025). These AFM images present the same pattern in respect to the size and crystals with those of Rasheed et al., (2020) for cellulose nanocrystals (CNC) extracted from bamboo (perennial grass) fibres and by Ahmima et al., (2024) for cellulosic micro/nanofibers (CNFs) extracted from *Lygea spartum* grass.

Conclusions

This study provides solid evidence over NC successful recovery from the *Phalaris aquatica* L., that gains continuously attention the last decade for its role as a second-generation energy crop. This is a native species of Mediterranean region and can contribute substantially to the biodiversity conservation through its valorisation, providing a range of products in a modern biorefinery. This biomass chemical treatment with NaOH followed by $NaClO_2$ removed the majority of amorphous cell wall components (hemicellulose and lignin), as supported from the cellulose increased content (from 43.1% to 90.5%), and the crystallinity index (from 59.1% to 76.1%). These results are highly encouraging, as they indicate that fewer delignification steps are required, in comparison with other lignocellulosic feedstocks. The extracted nanocellulose exhibited enhanced thermal stability, rendering it an excellent reinforcing agent for bio-nanocomposites in various industrial applications. These results provide an alternative route for a biorefinery, targeting except to fuels to the utilisation of biomass for bio-based materials sustainable production.

Declarations

Author Contribution

Dr Pappas was responsible for the conseptualisation, experiments and the initial data collection.Both authors drafted the work or revised it critically for important intellectual content; approved the version to be published.

Acknowledgements

Dr Ioannis A. Pappas would like to acknowledge Greek State Scholarships Foundation for financial support during his PhD research.

Data Availability

All data supporting the findings of this study are available within the paper. Any additional information will be available upon a request.

References

1. Abraham, E., Deepa, B., Pothan, L.A., Jacob, M., Thomas, S., Cvelbar, U., & Anandjiwala, R. (2011). Extraction of nanocellulose fibrils from lignocellulosic fibres: A novel approach. *Carbohydrate Polymers*, *86*(4), 1468-1475.
2. Abraham, E., Deepa, B., Pothen, L.A., Cintil, J., Thomas, S., John, M.J., Anandjiwala, R., & Narine, S.S. (2013). Environmental friendly method for the extraction of coir fibre and isolation of nanofibre.

Carbohydrate Polymers, *92*(2), 1477-1483.

3. Alemdar, A., & Sain, M. (2008). Biocomposites from wheat straw nanofibers: Morphology, thermal and mechanical properties. *Composites Science and Technology, 68*(2), 557–565.
4. Ben Sghaier, A.E.O., Chaabouni, Y., Msahli, S., & Sakli, F. (2012). Morphological and crystalline characterization of NaOH and NaOCl treated Agave Americana L. fiber. *Industrial Crops and Products*, *36*(1), 257-266.
5. Benini, K.C.C.d.C., Voorwald, H.G.C., Cioffi, M.O.H., Rezende, M.C.R., & Arantes, V. (2018). Preparation of nanocellulose from Imperata brasiliensis grass using Taguchi method. *Carbohydrate Polymers*, *192*, 337-346.
6. Brinchi, L., Cotana, F., Fortunati, E., & Kenny, J.M. (2013). Production of nanocrystalline cellulose from lignocellulosic biomass: Technology and applications. *Carbohydrate Polymers*, *94*(1), 154-169.
7. Carter, N., Grant, I., Dewey, M., Bourque, M. & Neivandt, D.J. (2021). Production and Characterization of Cellulose Nanofiber Slurries and Sheets for Biomedical Applications. *Frontier Nanotechnology* 3:729743. doi: 10.3389/fnano.2021.729743.
8. Deepa, B., Abraham, E., Cherian, B.M., Bismarck, A., Blaker, J.J., Pothan, L.A., Leao, A.L., de Souza, S.F., & Kottaisamy, M. (2011). Structure, morphology and thermal characteristics of banana nanofibers obtained by steam explosion. *Bioresource Technology*, *102*(2), 1988-1997.
9. Dini-Papanastasi, O., & Goulas, C.K. (1995). Variation of the number of flowering stems and its effect on forage yield in a population of *Phalaris aquatica* L. in Greece. *Options Mediterraneennes, 12*, 53-56.
10. European Commission: Directorate-General for Research and Innovation, Biodiversity and nature-based solutions – Analysis of EU-funded projects, Publications Office of the European Union, 2020, https://data.europa.eu/doi/10.2777/183298
11. Fahma, F., Iwamoto, S., Hori, N., Iwata, T., & Takemura, A. (2010). Isolation, preparation, and characterization of nanofibers from oil palm empty-fruit-bunch (OPEFB). *Cellulose*, *17*(5), 977-985.
12. Flauzino Neto, W.P., Silverio, H.A., Dantas, N.O., & Pasquini D. (2013). Extraction and characterization of cellulose nanocrystals from agro-industrial residueSoy hulls. *Industrial Crops and Products*, *42*,480-488.
13. Ghaemi, F., Abdullah, L. C., & Ariffin, H. (2019). Lignocellulose structure and the effect on nanocellulose production. In Lignocellulose for Future Bioeconomy (pp. 17–30). Elsevier.
14. Habibi, Y., Lucia, L.A., & Rojas O.J. (2010). Cellulose Nanocrystals: Chemistry, Self-Assembly, and Applications. *Chem. Rev.* 2010, 110, 6, 3479-3500.
15. Hamad, W.Y., & Hu, T.Q. (2010). Structure–process-Yield interrelations in nanocrystalline cellulose extraction. *The Canadian Journal of Chemical Engineering*, *88*(3), 392-402.
16. Hoseinpour, Z., Niazmand, R., Heydari-Majd, M. (2025). Extraction and characterization of nanocellulose from Cuminum cyminum L. husk by ball-milling-assisted ultrasound. *Carbohydrate Polymer Technologies And Applications,1,*100934.

17. Hsu, T.C., Guo, G.L., Chen, W.H., & Hwang, W.S., (2010). Effect of dilute acid pretreatment of rice straw on structural properties and enzymatic hydrolysis. *Bioresoure Technology*, *101*(13), 4907-4913.
18. Jeguirim, M., Dorge, S., & Trouvi, G. (2010). Thermogravimetric analysis and emission characteristics of two energy crops in air atmosphere: *Arundo donax* and *Miscanthus* giganthus. *Bioresource Technology*, *101*(2), 788-793.
19. Jiang, F., & Hsieh, Y.L. (2013). Chemically and mechanically isolated nanocellulose and their self-assembled structures. *Carbohydrate Polymers*, *95*(1), 32-40.
20. Johar, N., Ahmad, I., & Dufresne, A. (2012). Extraction, preparation and characterization of cellulose fibres and nanocrystals from rice husk. *Industrial Crops and Products*, *37*(1), 93-99.
21. Kabir, M.M., Wang, H., Lau, K.T., & Cardona, F. (2013). Effects of chemical treatments on hemp fibre structure. *Applied Surface Science*, *276*(1), 13-23.
22. Kargarzadeh, H., Ahmad, I., Abdullah, I., Dufresne, A., Zainudin, S.Y. & Sheltami, R.M. (2012). Effects of hydrolysis conditions on the morphology, crystallinity, and thermal stability of cellulose nanocrystals extracted from kenaf bast fibers. *Cellulose*, *19*, 855-866.
23. Kaushik, A., Singh, M., & Verma, G. (2010). Green nanocomposites based on thermoplastic starch and steam exploded cellulose nanofibrils from wheat straw. *Carbohydrate Polymers*, *82*(2), 337-345.
24. Kijo-Kleczkowska, A., Szumera, M., Gnatowski, A., & Sadkowski, D. (2022). Comparative thermal analysis of coal fuels, biomass, fly ash and polyamide. *Energy,258,*124840.
25. Langari, M.M., Nikzad, M., & Labidi, J. (2023). Nanocellulose-based sensors in medical/clinical applications: The state-of-the-art review. *Carbohydrate Polymers*, *304*, 120509.
26. Le Troedec, M., Sedan, D., Peyratout, C., Bonnet, J., Smith, A., Guinebretiere, R., Gloaguen, V., & Krausz, P. (2008). Influence of various chemical treatments on the composition and structure of hemp fibers. *Composites Part A-Applied Science and Manufacturing*, *39*(3), 514-522.
27. Li, R., Fei, J., Cai, Y., Li, Y., Feng, J., & Yao, J. (2009). Cellulose whiskers extracted from mulberry: A novel biomass production. *Carbohydrate Polymers*, *76*(1), 94-99.
28. Ljungberg, N., Cavaille, J.Y., & Heux, L. (2006). Nanocomposites of isotactic polypropylene reinforced with rod-like cellulose whiskers. *Polymer*,*47*(18), 6285-6292.
29. Lou, Z., Zhang, Y., Li, Y., & Xu, L. (2023). Study on microscopic physical and chemical properties of biomass materials by AFM. Journal of Materials Research and Technology, 2 4: 10005 -10026.
30. Lyons, G.A., McRoberts, C., Shekhar Sharma, H., McCormack, R., Carmichael, E. & McCall, R.D., (2013). Rapid analysis of purified cellulose extracted from perennial ryegrass (*Lolium perenne)* by instrumental analysis. *Bioresource Technology*, *146*,184-191.
31. Mandal, A., & Chakrabarty, D. (2011). Isolation of nanocellulose from waste sugarcane bagasse (SCB) and its characterization. *Carbohydrate Polymers, 86*(3), 1291-1299.
32. Maren, R., & William, T.W., 2004. Effect of sulfate groups from sulfuric acid hydrolysis on the thermal degradation behavior of bacterial cellulose. *Biomacromolecules, 5*(5), 1671-1677.

33. Mokhena, T.C., & John, M. J. (2020). Cellulose Nanomaterials: New Generation Materials for Solving Global Issues. *Cellulose* 27, 1149–1194. doi:10.1007/s10570-019-02889-w.
34. Moran, J.I., Alvarez, V.A., Cyras, V.P., & Vazquez, A. (2008). Extraction of cellulose and preparation of nanocellulose from sisal fibers. *Cellulose*, *15*(1), 149-159.
35. Norton, M.R., Lelievre, F. & Volaire, F. (2012). Summer dormancy in *Phalaris aquatica* L., the influence of season of sowing and summer moisture regime on two contrasting cultivars. *Journal of Agronomy and Crop Science*, *198*, 1-13.
36. Oh, H-J., Lee J-H., Jeong, Y., Kim, Y-J., & Chi, C-S. (2005). Microstructural characterization of biomedical titanium oxide film fabricated by electrochemical method. *Surface & Coatings Technology 198,* 247-252.
37. Oksman, K., Etang, J.A., Mathew, A.P., & Jonoobi, M. (2011). Cellulose nanowhiskers separated from a bio-residue from wood bioethanol production. *Biomass and Bioenergy*, *35*(1), 146-152.
38. Oliveira, D.M., Mota, T.R., Grandis, A., de Morais, Gutierrez R., de Lucas R.C., Polizeli, M.L.T.M., Marchiosi, R., Buckeridge M.S., Ferrarese-Filho,O., & dos Santos, W.D. (2020). Lignin plays a key role in determining biomass recalcitrance in forage grasses. Renewable Energy 147(I) 2206-2217.
39. Oram, R.N., Ferreira, V., Culvenor, R.A., Hopkins, A.A. & Stewart, A. (2009). The first century of *Phalaris aquatica* L. cultivation and genetic improvement: a review. *Crop Pasture Science*, *60*, 1–15.
40. Pappas, I.A. (2010). Assessment of range plants growth potential and their development for bioenergy production (Ph.D. Thesis). Faculty of Forestry and Natural Environment, Aristotle University, Thessaloniki, Greece. doi:http://dx.doi.org/10.12681/eadd/27517.
41. Pappas, I.A., Koukoura, Z., Tananaki, Ch., & Goulas, Ch. (2014). Effect of dilute acid pretreatment severity on the bioconversion efficiency of *Phalaris aquatica* L. lignocellulosic biomass into fermentable sugars. *Bioresource Technology*, *166*, 395-402.
42. Pappas, I.A., Papaioannou, E., & Koukoura, Z. (2023). Long term study of cell wall saccharification and high added value phenolic acids production from *Phalaris aquatica* L. energy crop. *Biomass and Bioenergy*, *177*, 16931.
43. Pascoli, D.U., Dichiara, A., Gustafson, R., & Renata, B. (2023). A Robust Process to Produce Lignocellulosic Nanofibers from Corn Stover, Reed Canary Grass, and Industrial Hemp. *Polymers, 15*, 937. https:// doi.org/10.3390/polym15040937.
44. Patil, T.V., Patel, D.K., Dutta, S.D., Ganguly, K., Santra, T.S., & Lim, K.T. (2023). Nanocellulose, a versatile platform: From the delivery of active molecules to tissue engineering applications. *Bioactive Materials, 9*, 566-589.
45. Pires, J.R.A., Souza, V.G.L., & Fernando, A.L. (2019). Valorization of energy crops as a source for nanocellulose production – Current knowledge and future prospects. *Industrial Crops and Products,140,*111642.
46. Pires, J.R.A., Souza, V.G.L., Gomes, L.A., Coelhoso, I.M., Godinho, M.H., & Fernando, A.L. (2022). Micro and nanocellulose extracted from energy crops as reinforcement agents in chitosan films. *Industrial Crops and Products,186,*115247.

47. Rasheed, M., Jawaid, M., Parveez, B., Zuriyati, A., & Khan, A. (2020). Morphological, chemical and thermal analysis of cellulose nanocrystals extracted from bamboo fibre. Int J Biol Macromol (International Journal of Biological Macromolecules), 160:183-191.
48. Rehman, N., de Miranda, M.I.G., Rosa, S.M.L.,Pimentel, D.M., Nachtigall, S.M.B., & Bica, C.I.D. (2014). Cellulose and nanocellulose from maize straw: An insight on the crystal properties. *Journal of Polymers and the Environment*, *22*(2), 252-259. Rosa, M.F., Medeiros, E.S., Malmonge, J.A., Gregorski, K.S., Wood, D.F., Mattoso, L.H.C., Glenn, G., Orts, W.J., & Imam, S.H. (2010). Cellulose nanowhiskers from coconut husk fibers: Effect of preparation conditions on their thermal and morphological behaviour. *Carbohydrate Polymers*, *81*(1), 83-92.
49. Rosa, S.M.L., Rehman, N., De Miranda, M.I.G., Nachtigall, S.M.B., & Bica, C.I.D. (2012). Chlorine-free extraction of cellulose from rice husk and whisker isolation. *Carbohydrate Polymers*, *87*(2), 1131-1138.
50. Sanderson, M.A. & Adler, P.R. (2008). Perennial forages as second generation bioenergy crops. *International Journal of Molecular Sciences, 9*, 768-788.
51. Sathwane, M., Deshmukh, R.K., Gaikwad, K.K., & Maji, P.K. (2024). Valorization of nanocellulose from bael (Aegle marmelos correa) fruit waste shells: Surface chemistry and morphological analysis. *Bioresource Technology Reports*,*25*, 101727.
52. Segal, L., Creely, J., Martin, A., & Conrad, C. (1959). An empirical method for estimating the degree of crystallinity of native cellulose using the X-ray diffractometer. *Textile Research Journal*, *29*(10), 786-794.
53. Silverio, H.A., Flauzino Neto, W.P., Dantas, N.O., & Pasquini, D. (2013). Extraction and characterization of cellulose nanocrystals from corncob for application as reinforcing agent in nanocomposites. *Industrial Crops and Products,44*, 427-436.
54. Siro, I. & Plackett, D. (2010). Microfibrillated cellulose and new nanocomposite materials: a review. *Cellulose 17*, 459-494.
55. Song, Q., Winter, W.T., Bujanovic, B.M. & Amidon, T.E. (2014). Nanofibrillated Cellulose (NFC): A High-value co-product that improves the economics of cellulosic ethanol production. *Energies*, *7*, 607-618.
56. Srivastava, N., Singh, R., Srivastava, M., Mohammad, A., Harakeh, S., Singh, R. P., Pal, D. B., Haque, S., Tayeb, H.H., Moulay, M., & Gupta, V.K. (2023). Impact of nanomaterials on sustainable pretreatment of lignocellulosic biomass for biofuels production: An advanced approach. *Bioresource Technology 369 128471*.
57. Sucinda, E.F., Abdul Majid, M.S., Ridzuan, M.J.M., Sultan, M.T.H., & Gibson, A.F. (2020). Analysis and physicochemical properties of cellulose nanowhiskers from Pennisetum purpureum via different acid hydrolysis reaction time. *International Journal of Biological Macromolecules,155,* 241-248.
58. Thiripura Sundari, M., & Ramesh, A. (2012). Isolation and characterization of cellulose nanofibers from the aquatic weed water hyacinth-Eichhornia crassipes. *Carbohydrate Polymers*, *87*(2), 1701-1705.

59. Trivedi, A.K., Kumar, A., & Gupta M.K. (2023). Extraction of nanocellulose from wheat straw and its characterization. *Materials Today:Proceedings*,*78*, 48-54 .
60. Van Soest, P.J., Robertson, J.B., & Lewis, B.A. (1991). Methods for dietary fiber, Neutral detergent fiber and nonstarch polysaccharides in relation to animal nutri-tion. *Journal of Dairy Science*, *74*, 3583-3597.
61. Velázquez, M.E., Ferreiro, O.B., Menezes, D.B., Corrales-Ureña, Y., Vega-Baudrit, J.R., & Rivaldi, J.D. (2022). Nanocellulose Extracted from Paraguayan Residual Agro-Industrial Biomass: Extraction Process, Physicochemical and Morphological Characterization. *Sustainability,14*,11386. https://doi.org/10.3390/su141811386.
62. Viti, M. M., Gkimtsas, G., Liquete, C., Dubois, G., Borg, J., S. D Costa, Teller, A., Hauser, R, & Robuchon. M. (2024). Introducing the progress monitoring tools of the EU Biodiversity Strategy for 2030. Ecological Indicators 164, 112147.
63. Yang, H., Yan, R., Chen, H., Lee, D.H., & Zheng, C. (2007). Characteristics of hemicellulose, cellulose and lignin pyrolysis. *Fuel*, *86* (12-13), 1781-1788.
64. Zhang, Q., Ma, R., Ma, L., Zhang, L., Fan, Y., & Wang, Z. (2021). Contribution of lignin in esterified lignocellulose nanofibers (LCNFs) prepared by deep eutectic solvent treatment to the interface compatibility of LCNF/PLA composites. *Ind. Crop. Prod. 166,* 113460 https://doi.org/10.1016/j.indcrop.2021.113460.
65. Zhang, F., Shen, R., Yang, X., & Lin, D. (2023). Nanocellulose: An amazing nanomaterial with diverse applications in food science. *Carbohydrate Polymers*, *304*, 120497.

Tables

Table 1. Chemical composition (% w/w dry weight) of *Phalaris aquatica* L. fibres at the end of each stage of chemical treatment

Composition (%)	Raw fibres	NaOH treatment	Bleaching treatment
Cellulose	43.1±3.1	77.7±1.8	90.5±1.5
Hemicellulose	25.8 ± 2.3	13.6±1.2	8.9±0.6
Lignin (%)	7.6±1.4	6.5±0.4	0.4±0.1

Table 2. Crystallinity index (CrI) of *Phalaris aquatica* fibres at different stages of chemical treatment

Sample	Crystallinity index (%)
Raw fibres	59.1
NaOH treatment	66.3
Bleaching treatment	67.0
NanoCellulose (NC)	76.1

Figures

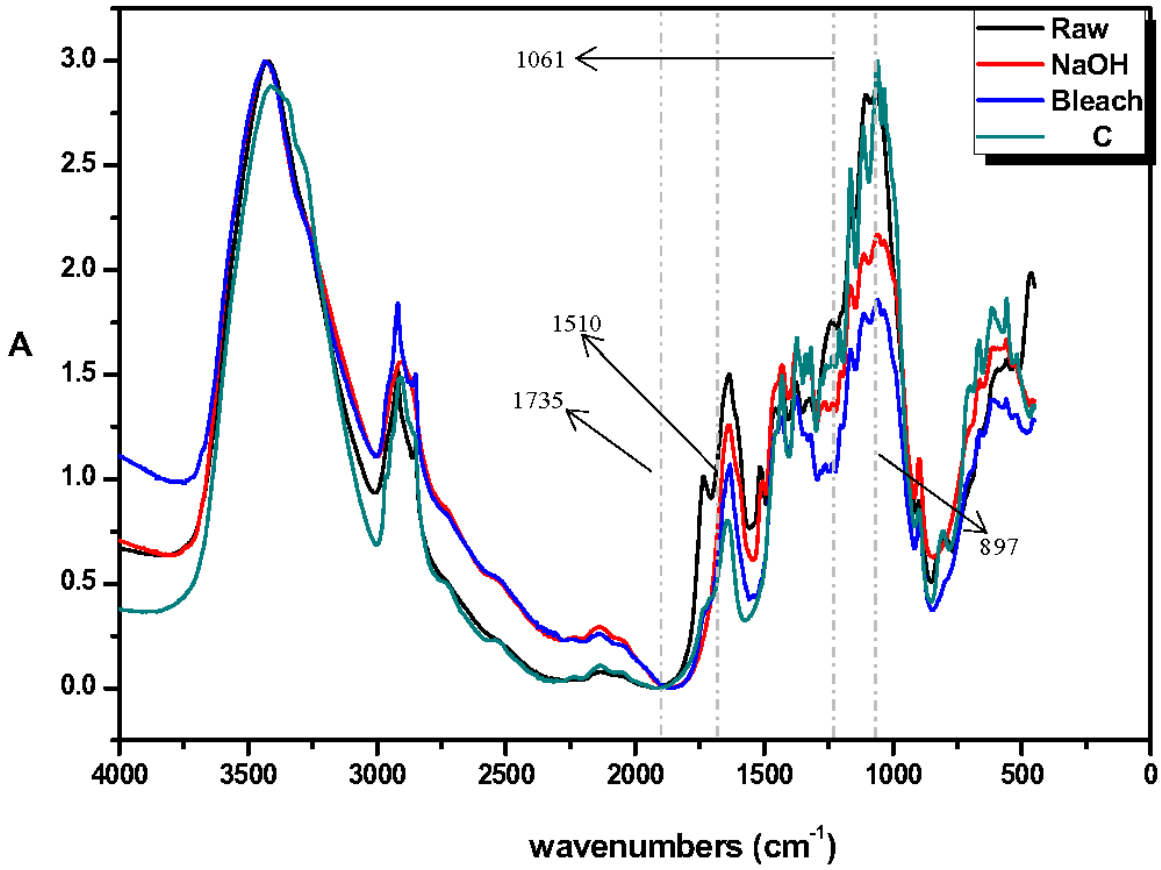


Figure 1. FTIR spectra of (a) raw biomass; (b) alkali treated; (c) bleached and (d) acid hydrolysed cellulose of *Phalaris aquatica*.

Figure 1

See image above for figure legend.

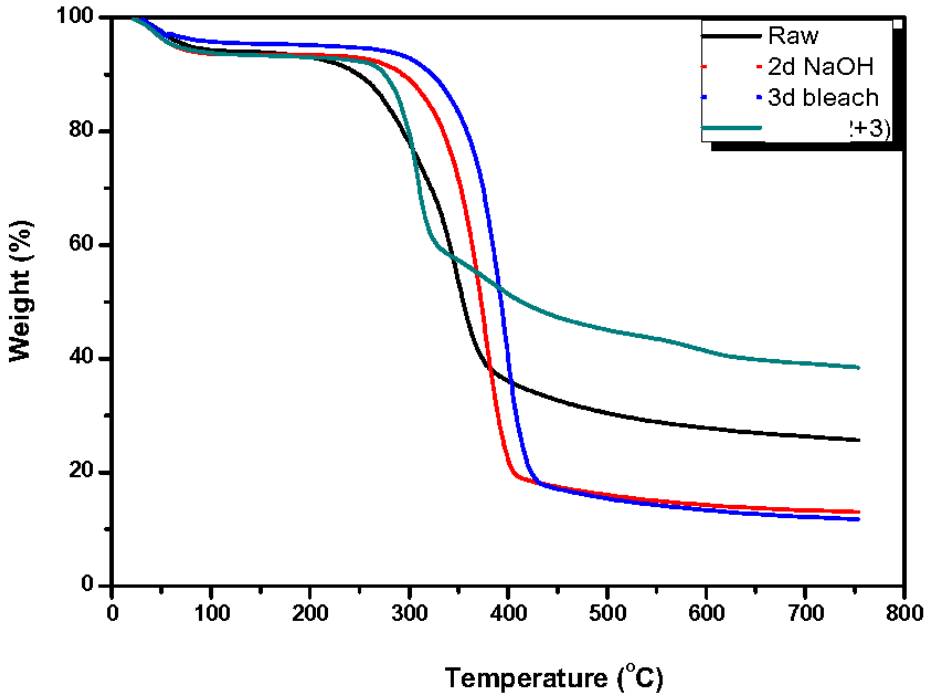


Figure 2. TGA of (a) raw biomass; (b) alkali treated; (c) bleached and (d) acid hydrolysed cellulose of *Phalaris aquatica*.

Figure 2

See image above for figure legend.

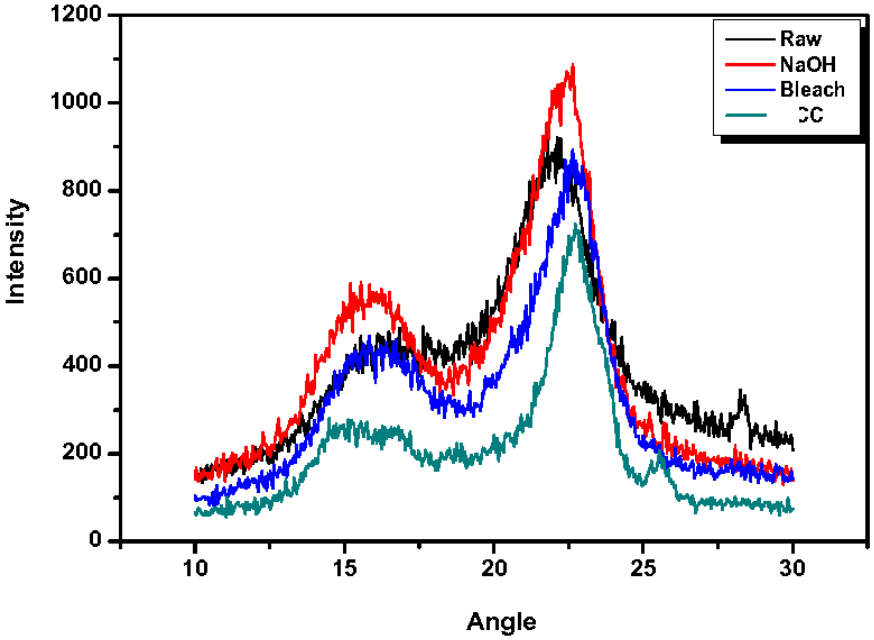


Figure 3. X-ray diffraction patterns for (a) raw biomass, (b) NaOH (alkali)-treated biomass, (c) $NaClO_2$ (bleached) biomass and (d) acid hydrolysed cellulose.

Figure 3

See image above for figure legend.

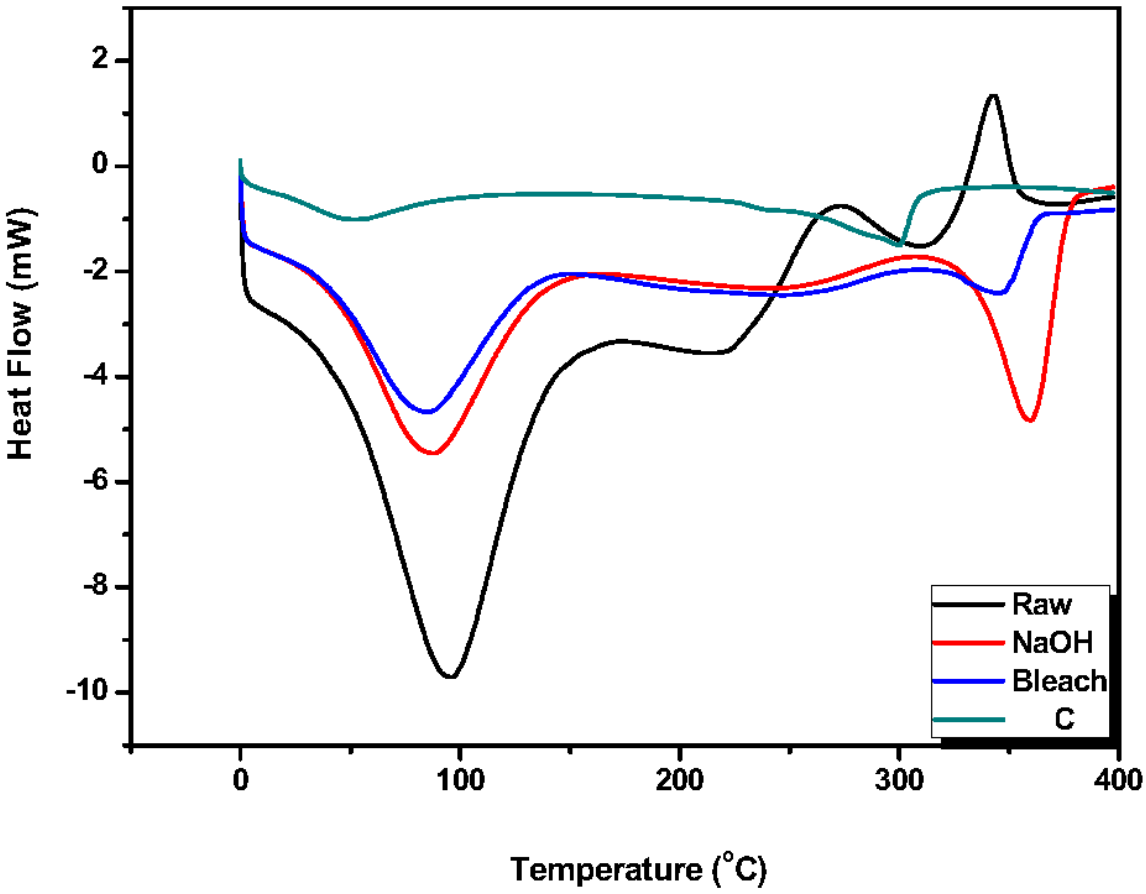


Figure 4. DSC curve of (a) raw; (b) alkali treated, (c) bleached treated and (d) acid hydrolysed cellulose.

Figure 4

See image above for figure legend.

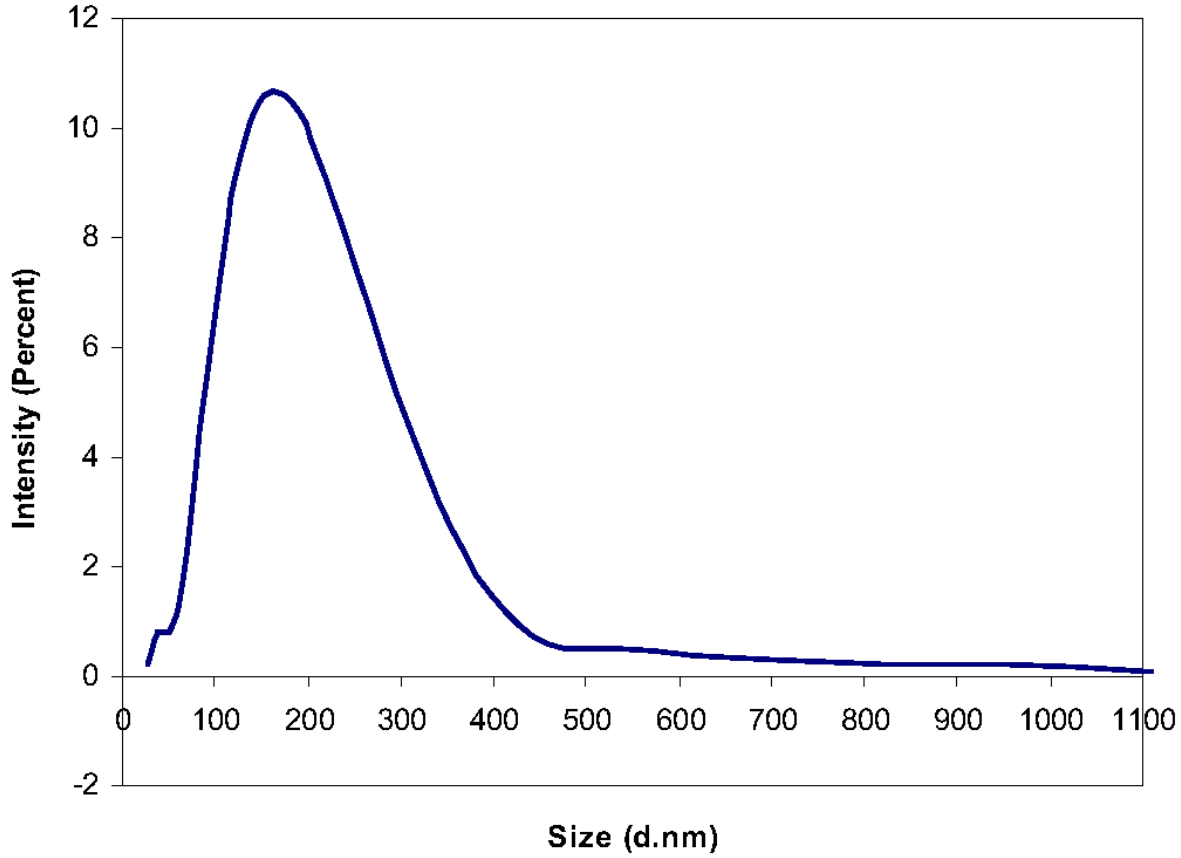


Figure 5. Particle size distribution of NC aggregates obtained from *Phalaris aquatica*.

Figure 5

See image above for figure legend.

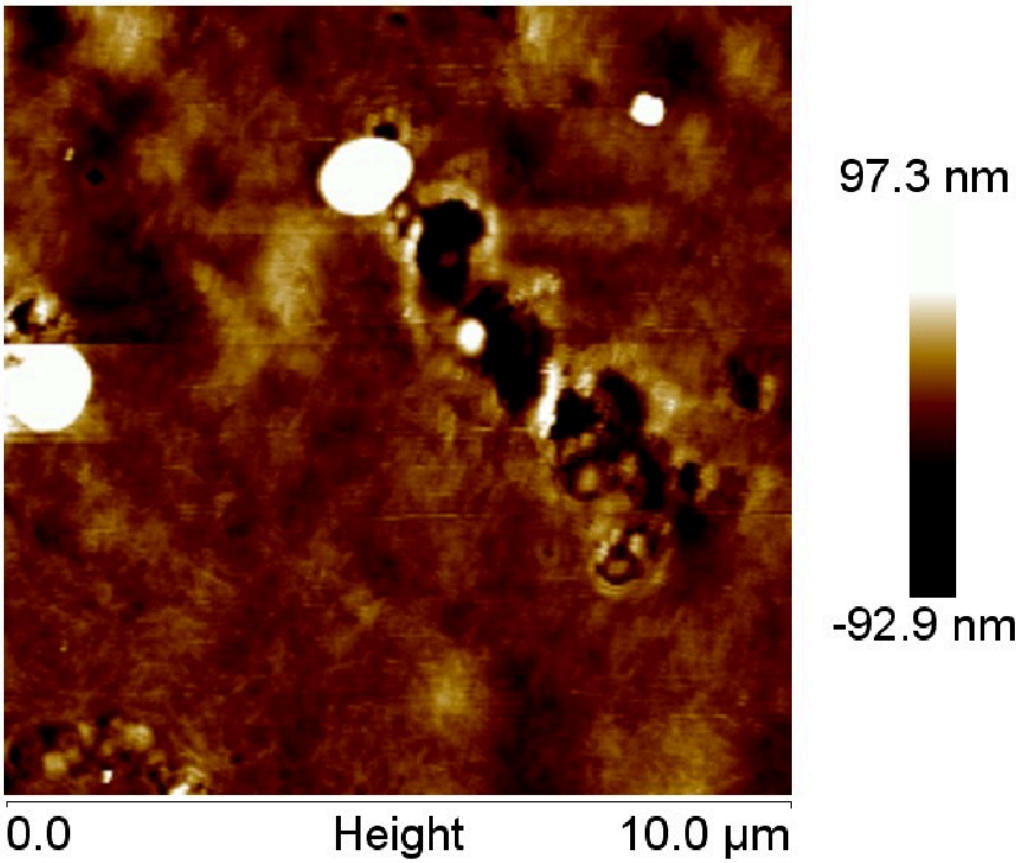


Figure 6. Atomic Force Microscopy (AFM) of acid hydrolysed cellulose of *Phalaris aquatica* L.

Figure 6

See image above for figure legend.